

Article

Engineering Characteristics of SBS/Nano-Silica-Modified Hot Mix Asphalt Mixtures and Modeling Techniques for Rutting

Inamullah Khan ^{1,*}, Abdul Wahab Khattak ¹, Alireza Bahrami ^{2,*}, Shahab Khattak ³ and Ali Ejaz ¹

¹ Transportation Engineering Department, National Institute of Transportation, National University of Sciences and Technology, Islamabad 44000, Pakistan

² Department of Building Engineering, Energy Systems and Sustainability Science, Faculty of Engineering and Sustainable Development, University of Gävle, 801 76 Gävle, Sweden

³ Transportation Engineering Department, Abasyn University, Peshawar 25100, Pakistan

* Correspondence: inamullah.khan@nit.nust.edu.pk (I.K.); alireza.bahrami@hig.se (A.B.)

Abstract: Flexible pavements are mostly affected by meteorological factors in addition to traffic loads, which results in premature pavement failures like rutting and moisture-induced damage. This study focuses on the impacts of adding various contents of nano-silica (NS), i.e., 2%, 4%, 6%, and 8% (percentage weight of asphalt), along with a constant value of 4.5% styrene-butadiene-styrene (SBS). To assess the effectiveness of modified and unmodified mixtures, the indirect tensile strength (ITS) test, resilient modulus (MR) test, and wheel tracking test were conducted. The MR test was performed at dual temperature values, i.e., 25 °C and 40 °C, and demonstrated different metrological conditions in this region. The tensile strength ratio was used to estimate the mitigation of water losses in hot mix asphalt (HMA) mixtures (specimens) utilizing ITS test results of the conditioned and unconditioned specimens. Moreover, a model was developed for the rutting potential of the modified specimens using multi expression programming (MEP), a sophisticated technique that employs experimental data and suggests an equation for different input variables. The results indicated that the addition of NS to SBS-modified bitumen enhanced different mechanical properties of the specimens, including the stiffness and moisture and rutting resistances. The temperature had adverse effects on the stiffness of the specimens, while the modifiers had a direct relationship with the stiffness. The two-way factorial method justified the effect of the temperature and modifiers on MR with 95% precision, while the MEP model for rutting showed an R^2 value of >0.95 , which revealed a good relationship between the experimental and predicted data. Furthermore, NS and SBS had a good impact on the mechanical properties of the HMA specimens.

Keywords: asphalt; pavement; styrene-butadiene-styrene; nano-silica optimization; indirect tensile strength test; resilient modulus; wheel tracking test; stiffness; rutting resistance; modeling



Citation: Khan, I.; Khattak, A.W.; Bahrami, A.; Khattak, S.; Ejaz, A. Engineering Characteristics of SBS/Nano-Silica-Modified Hot Mix Asphalt Mixtures and Modeling Techniques for Rutting. *Buildings* **2023**, *13*, 2352. <https://doi.org/10.3390/buildings13092352>

Academic Editor: Paulo Cachim

Received: 22 July 2023

Revised: 28 August 2023

Accepted: 31 August 2023

Published: 15 September 2023



Copyright: © 2023 by the authors. Licensee MDPI, Basel, Switzerland. This article is an open access article distributed under the terms and conditions of the Creative Commons Attribution (CC BY) license (<https://creativecommons.org/licenses/by/4.0/>).

1. Introduction

The necessity for long-lasting pavements with minimum maintenance and rehabilitation costs has caused a spike in demand for high-quality bitumen in recent years. Rutting and moisture damage are the two most frequently occurring distresses of flexible pavements. To mitigate and minimize these distresses, several methods are used, including polymer and nano-material composite modifications [1]. Degradation of the toughness and durability of hot mix asphalt (HMA) mixtures is known as water damage [2]. Rutting is the depression of pavements under repeated axle loads in the wheel path areas of a road [3–5].

The different methods of polymer modifications to enhance the bitumen performance against multiple distresses include polymer modifications of bitumen like styrene-butadiene-styrene (SBS), rubber, styrene-butadiene rubber (SBR), and Elvaloy [6]. The impact of SBS, nano-silica (NS), and SBS/NS composites was evaluated via the linear amplitude sweep (LAS) test and the four-point flexural binding test, which indicated increased fatigue life at optimum levels of 6% of NS and 5% of SBS [7]. The effect of NS on

polymer-modified bitumen mixtures was assessed via resilient modulus (MR) and dynamic creep tests, which demonstrated improved age reduction and enhancement in the fatigue and permanent deformation resistance with decreased water sensitivity [8]. The influence of an SBS-modified asphalt mixture with 4.5% optimum content was examined for storage and performance, which concluded that bitumen lost its performance significantly at high temperatures while storability was improved with the use of SBS [9]. A case study was conducted to determine the impact of NS on a polypropylene-modified bitumen mixture via the four-point beam test, fatigue test, indirect tensile strength (ITS) test, and stiffness modulus test, with the conclusion of noticeable effects on the performance of the modified HMA [10]. The influence of NS on premixed polyethylene glycol and methylene diphenyl diisocyanate was analyzed through the dynamic shear rheometer (DSR) test which enhanced the resistance against rutting and fatigue [11].

The nano-materials that are used as binder modifiers include nano-clay (NC), carbon nano-tubes, carbon nano-fibers, graphene nano-platelets, graphene oxide, nano-lime, NS, nano-TiO₂, nano-ZnO, and nano-fly ash [12]. The impact of NS on polymer-modified bitumen (PMB) was investigated by DSR, X-ray diffraction, and scanning electron microscopy, which resulted in finding that adding NS to PMB delayed aging with no crystalline phase while extreme heat marked an improvement in complex modulus and a decline at low temperatures, which increased the resistance against rutting and fatigue [13]. The influence of NS on low-temperature cracks (LTCs) and medium-temperature cracks (MTCs) under freeze/thaw circumstances was studied by semi-circular bending and edge-notched disc bending tests, illustrating that NS improved the long-term performance of LTCs and MTCs [14]. Moreover, the combined effects of NS and polyethene terephthalate (PET) were evaluated via the wheel tracking test (WTT), ITS test, MR test, and drain-off test, which showed that 4–8% of NS and 6% of PET enhanced the rutting and fatigue resistances, stiffness modulus, and tensile strength ratio (TSR) [15]. The impact of NS was assessed on modified mixtures, which was concluded that softening and viscosity were increased along with an improvement in the fatigue life and a decrease in the moisture susceptibility [16]. NS, bentonite, and zerovalent iron were used as additives in asphalt mixtures, with improved fatigue and permanent deformation obtained due to NS and bentonite, while the water resistance was low owing to zerovalent iron [17]. Accordingly, for the moisture resistance, the equilibrium between the adhesion and de-bonding processes occurring at the binder–aggregate interface could only be achieved with a high degree of cohesion [18]. The effect of NS on modified HMA was assessed by the modified Lottman test for the moisture susceptibility; the results indicated a 26.25% improvement in the moisture resistance [19]. Adding nano-particles like NC and NS to asphalt decreased the flowability of bitumen binder and caused the permanent deformation and fatigue resistance in asphalt mixtures, while SBS also improved the rutting and thermal cracking resistances [20]. Different models were developed for the rut depth and rheological parameters based on the finite element method. The rheological parameters were verified utilizing a French pavement rutting tester, and the results displayed that viscosity and elasticity coefficient had a considerable effect on the rut depth [19,20].

Previous studies were mostly concentrated on the binder modification and its rheological properties, while the objective of this research was the optimization of NS with 4.5% constant SBS-modified bitumen mixtures. The HMA mixture performance is primarily determined by the stiffness, rutting, and moisture susceptibility.

This study has been divided into two main sections. The first section investigates the performance of SBS/NS-modified bitumen mixtures (specimens) with regard to the stiffness, rutting, and moisture susceptibility using constant 4.5% SBS and different percentages of NS (2%, 4%, 6%, and 8%) by weight of bitumen. The second section encompasses the development of models using different artificial intelligence (AI) techniques and statistical analysis.

2. Methodology and Experimental Tests

2.1. Materials and Preparation of Specimens

This research made use of 60–70 penetration grade bitumen procured from Attock Oil Refinery Limited, given in Table 1. Aggregates were provided from Babuzai Crush Plant, Pakistan, having a nominal maximum aggregate size (NMAS) of 19 mm in accordance with the National Highway Authority (NHA)-B gradation, as listed in Table 2. The properties of aggregates are presented in Table 3. Linear SBS was imported from Shijiazhuang Tuya Company, China, with properties provided in Table 4. NS was purchased from a lab zone in Peshawar, Pakistan, with its properties indicated in Table 5.

Table 1. Properties of bitumen.

Test Description	Result	Specification	Standard
Penetration test @ 25 °C (mm)	66	60–70	ASTM 5
Flash point test (°C)	254	232 (Min)	ASTM D 92
Fire point test (°C)	300	270 (Min)	ASTM D 92
Specific gravity test	1.03	1.01–1.06	ASTM D 70
Softening point test (°C)	50.4	49–56	ASTM D 36-06
Ductility test (cm)	107	100 (Min)	ASTM D113-99

Table 2. NHA-B gradation NMAS (19 mm).

Sieve Size	19	12.5	9.5	4.75	2.38	1.18	0.075	Pan
NHA-B specification	100	75–90	60–80	40–60	20–40	5–15	3–8	-
Our selection	100	82.5	70	50	30	10	5.5	-

Table 3. Properties of aggregates.

Type of Test	Results (%)	Specification	Standard	
Fractured particles	99	90% (Min)	ASTM D-5821	
Los Angeles abrasion	20.3	30% (Max)	ASTM C-131	
Flakiness of aggregates	4.8	10% (Max)	ASTM D-4791	
Elongation index of aggregates	4.7	10% (Max)	ASTM D-4791	
Impact value of aggregates	16.23	30% (Max)	BS-812	
Crushing value of aggregates	18.52	30% (Max)	BS-812	
Water absorption	Fine aggregates	2.53	3% (Max)	ASTM C-128
	Coarse aggregates	0.80	3% (Max)	ASTM C-127
Specific gravity	Fine aggregates	2.626	-	ASTM C-128
	Coarse aggregates	2.633	-	ASTM C-127
Clay percentage	Coarse aggregates	0.565	-	ASTM C-142
	Fine aggregates	2.815	-	ASTM C-142

The specimens were prepared in two phases: first, additives were added to 60–70 grade bitumen using a shear mixer of 3000 revolutions/min (rpm) at 163 °C [13]. The purpose of the Marshal mix design was to obtain optimum binder content (OBC), which resulted in 4.25% OBC at 4% air voids. The bitumen specimens were cast utilizing a constant 4.5% SBS and different percentages of NS (2%, 4%, 6%, and 8%) by weight of bitumen. Subsequently, Marshal specimens were prepared for modified and unmodified bitumen for the MR and ITS tests, while Superpave gyratory specimens were made for WTT.

Table 4. Properties of SBS.

Description	Property
SBS type	SBS YH-791H
Structure	Linear
Purity	>95%
Appearance	White granules
Brand name	TY
Viscosity of 5% styrene solution at 25 °C	2.24 Pa·s
S/B	30%/70%
Tensile strength	20 MPa
Hardness	~76 A

Table 5. Properties of NS.

Name	Unit	Result
Chemical formula	-	SiO ₂
Microstructure shape	-	Spherical
SiO ₂ (dry basis)	%	>98
Specific surface area	m ² /gm	580
Average pore diameter	nm	7
Original particle size	nm	14–36
Grain size distribution	nm	<120
Bulk density	gm/cm ³	0.1–0.15
Tamping density	gm/cm ³	0.2–0.30
Temperature resistance	°C	1350
pH	-	6–7

2.2. MR Test

The MR test is considered as the main test for the design of flexible pavements and examines the correlation between subjected stress and regained strain under cyclic loading. The MR test was utilized to assess the stiffness of bitumen specimens due to dynamic stress and strain [21]. The MR test was used to ascertain whether incorporating NS would result in significant modifications in the resilience of the modified HMA specimens.

The tests were done at two different temperatures, i.e., 25 °C (room temperature) and 40 °C. The specimens' ITS test was conducted, and then the MR test was performed. The peak loading force utilized during the tests was 5–20% of the specimens' ITS because this would almost completely recover the deformation.

2.3. ITS Test

Rutting, cracking, water sensitivity, and stripping would be estimated by performing the ITS test. This test is normally conducted using a universal testing machine in conformity with ASTM D6391 [22]. Two salient features of the asphalt mixture can be determined by doing this test. The moisture susceptibility of asphalt is typically evaluated by comparing the specimens' ITS before and after conditioning in water to a standard test specimen. The cracking potential of HMA can also be examined by determining the tensile strain at failure. It is more likely that HMA with a high tensile strain until failure is more resistant to cracking. Figure 1 depicts an experimental test conducted in the laboratory. During this test, a cylindrical specimen was compressed along the vertical diametric plane. Loading strips with 0.5-inch width were utilized for 4-inch-diameter specimens with 2.5-inch height to ensure a uniform load distribution in a direction perpendicular to the load. For 4-inch-diameter specimens at 25 °C, a deformation rate of 50 mm per minute was prescribed, and for 6-inch-diameter specimens, the applied deformation rate was 76.2 mm per minute. This test measured the tensile strength of the HMA specimens, which affected the cracking behavior of the materials.

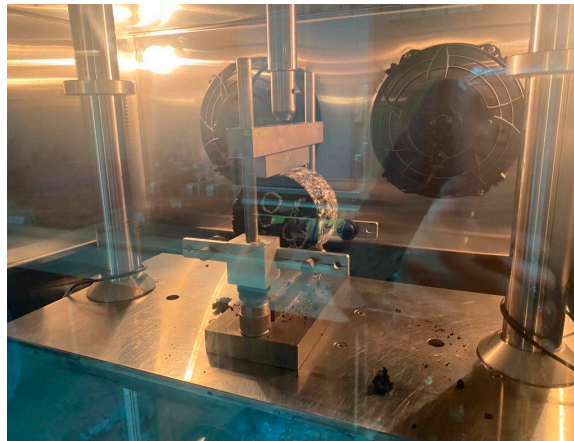


Figure 1. ITS test.

2.4. WTT

WTT is an experimental method that reciprocates loading cycles on the HMA specimens to investigate the rutting and stripping potential. In the test, a steel wheel weighing 158 lbs moved with a velocity of 52 ± 2 passes per minute across a pair of asphalt specimens dry or submerged in water at a temperature of 40 °C or 50 °C. A linear variable displacement transducer quantified rutting at 11 different points along the longitudinal wheel path with 0.01 mm precision. The purpose of WTT was to assess the rutting potential of the modified and unmodified bitumen specimens. The WTT instrument is illustrated in Figure 2.



Figure 2. WTT instrument.

3. Results and Discussion

3.1. Results of Binder Test

As mentioned earlier, a constant 4.5% SBS and different percentages of NS (2%, 4%, 6%, and 8%) by weight of bitumen were added to 60–70 grade penetration bitumen to enhance the permanent deformation and moisture resistance of the HMA specimens. To achieve this objective, the modified and unmodified bitumen specimens were tested for the consistency, i.e., penetration [23] and softening point [24]. Figure 3 shows the test results of the modified and unmodified specimens. The softening point was increased as the NS percentage rose, while the penetration was declined. The decrease in the penetration indicated an improvement in hardness at median temperatures and an enhancement in rutting at high temperatures. The absorption of bitumen light volatiles by NS was analogous to these results since NS fragments were stiffer than asphalt, causing a rise in the asphalt stiffness [25].

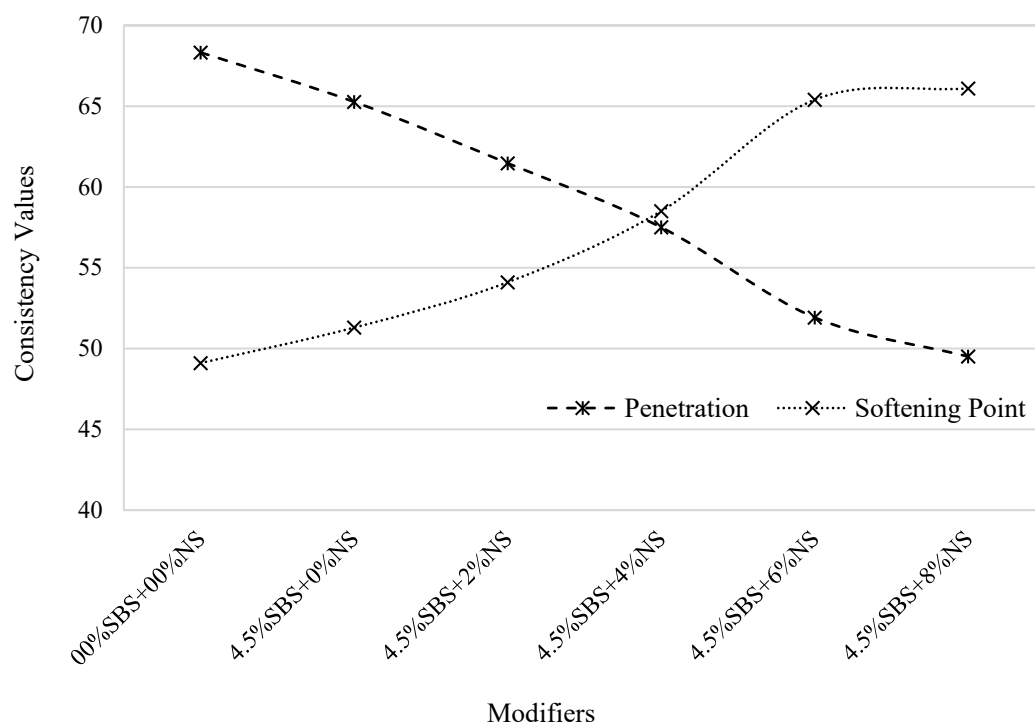


Figure 3. Effect of modifiers on consistency of bitumen.

3.2. Results of ITS Test

The HMA specimens were made for a base binder with asphalt modified with 0% SBS + 0% NS, 4.5% SBS + 0% NS, 4.5% SBS + 2% NS, 4.5% SBS + 4% NS, 4.5% SBS + 6% NS, and 4.5% SBS + 8% NS, according to the Marshall mix design [26]. The purpose of the modified Lottman test (AASHTO T283) is to measure the TSR value.

Subsequently, the moisture susceptibility was determined according to these test results. The results of the ITS test on the conditioned (C) and unconditioned (UC) specimens are displayed in Figure 4. The unmodified specimens resulted in the ITS values relative to the modified specimens. The experiment demonstrated that, up to 6% NS, the HMA specimens exhibited enhanced resistance to the stripping and moisture sensitivity. After that, the addition of NS had inverse effects. The results revealed that TSR of the unmodified HMA specimen was about 79%, while that of 4.5% SBS + 6% NS was about 97%. NS has a very small particle size with a large exposed area; that is why it replaces a large quantity of bitumen and improves the modified bitumen structure [27]. TSR was increased as the percentage of NS was increased up to 4.5% SBS + 6% NS, and then was decreased. This issue implied that NS and SBS significantly changed ITS of the specimens by developing a strong attractive force between asphalt and the aggregate surfaces. It signified that SBS with NS strengthened the adhesive and cohesive bonds among bitumen-coated aggregates in the specimens, leading to the development of better stripping and moisture resistance, which is also supported by research studies [28].

Figure 4 displays that the ITS values of the conditioned (C) specimens were lower than those of their unconditioned (UC) counterparts, which matches the results in the literature [8,29,30]. Lower ITS values in the conditioned specimens could be the outcome of the reduced cohesion in the specimens as a result of exposure to the moisture [10]. The smaller differences in the ITS values for the conditioned and unconditioned specimens demonstrated that the modifier material had better performance in extreme wet conditions.

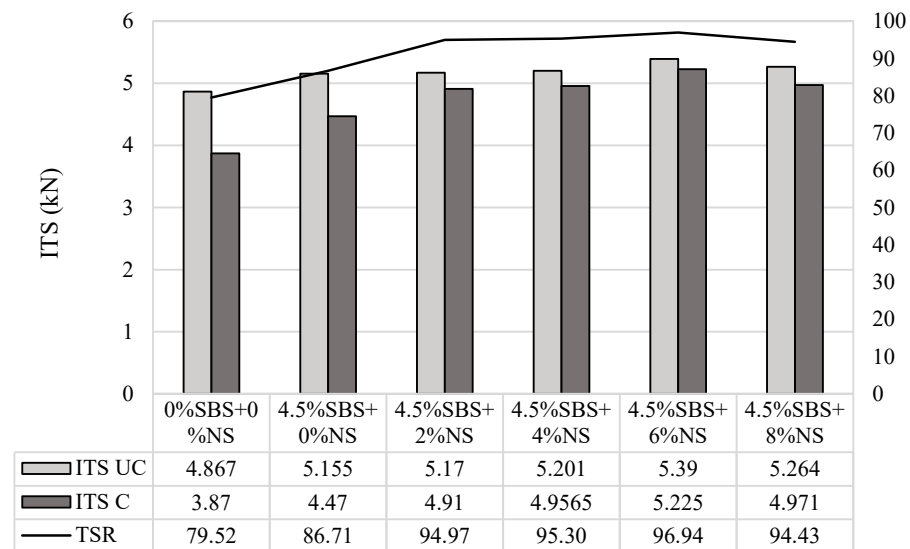


Figure 4. Results of ITS test.

3.3. Results of MR Test

Figure 5 depicts the results of the MR test for the specimens with various NS contents and a constant quantity of SBS. The modified HMA specimens exhibited a higher MR than the control specimen. It is noted that the MR values were enhanced from 1492 MPa for the specimen 4.5% SBS + 0% NS to 1940 MPa, 1944 MPa, and 2952 MPa for the specimens 4.5% SBS + 2% NS, 4.5% SBS + 4% NS, and 4.5% SBS + 6% NS, respectively, at 25 °C. At 40 °C, the MR values were increased from 1131 MPa for the specimen 4.5% SBS + 0% NS to 1345 MPa, 1385 MPa, and 2454 MPa for the specimens 4.5% SBS + 2% NS, 4.5% SBS + 4% NS, and 4.5% SBS + 6% NS, respectively. Moreover, the specimen 4.5% SBS + 8% NS yielded lower MR values, i.e., 2570 MPa at 25 °C and 2169 MPa at 40 °C. Therefore, the modified specimens provided increased resistance to the permanent pavement deformation, had a stronger load spreading ability, and had a higher load bearing capacity than the control specimens. A higher stiffness might be linked to the asphalt being modified with the nano-material and polymer, which enhanced effectiveness and the specimens' resistance at high temperatures and heavy axle loads. Another reason for the improvement in MR was the decreased flowability and adhesion among aggregates and asphalt while limiting the specimens' free flow [10].

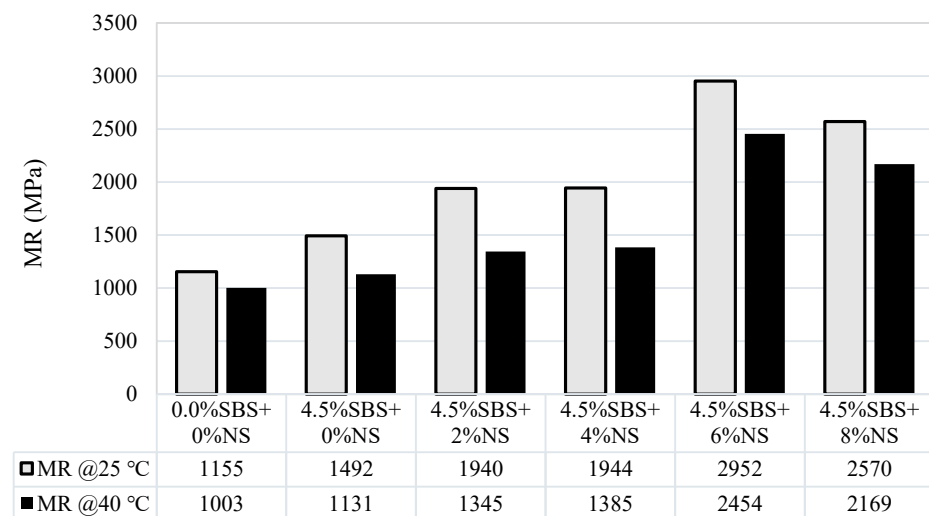


Figure 5. Results of MR test at 25 °C and 40 °C.

3.4. Results of WTT

Figure 6 illustrates the rutting potential of the specimens, in which the rutting resistance was improved as the NS content was increased to 6% and then it was decreased onward. This improvement is attributable to an increase in the adhesion force among bitumen and aggregates, which prevented aggregates from sinking under the influence of the axle load, hence reducing the rutting deformation [28]. The study indicated that adding NS to the specimens reduced rutting in comparison to the unmodified specimen and 4.5% SBS-modified HMA specimen. Moreover, adding 4.5% SBS was also effective as compared to the unmodified HMA specimen.

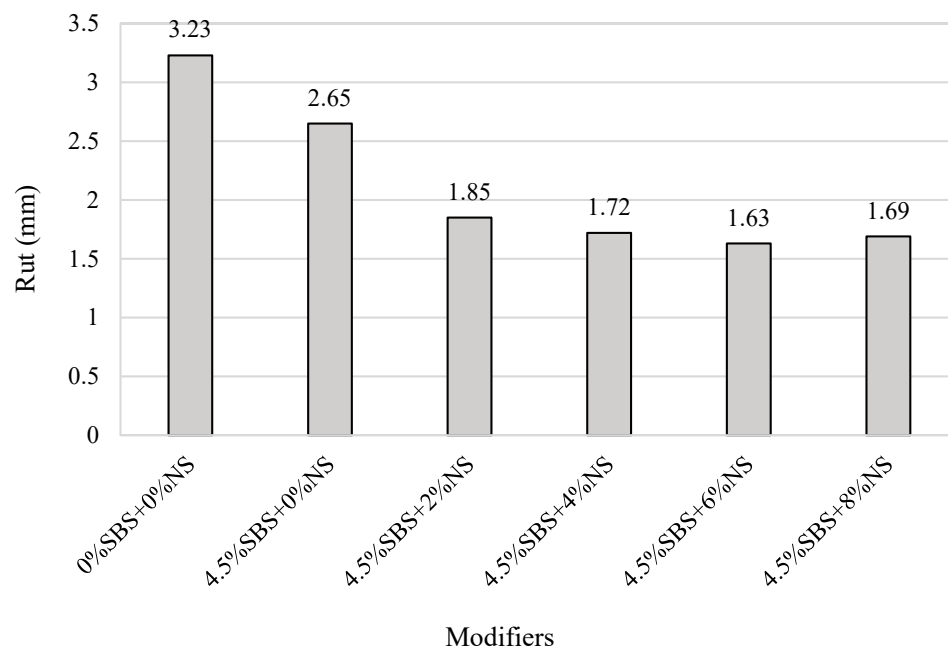


Figure 6. Results of WTT.

In contrast to the previous relevant research, this study elaborated on a more noticeable and similar impact of SBS with NS [23–25]. The research revealed that the modified HMA has improved resistance against accumulated deformation under high vehicle loads.

3.5. Experimental Design of MR

To examine the responsiveness of the dependent variables (MR) to the modifier and temperature, an experimental design, factorial design was utilized [26–28]. A mixture of several factors was used in the experimental design to check the effectiveness of such variables on the response variable. The experimental method's design was employed to reduce efforts. The concentration of the impact notion states that a few important variables affect the majority of activities, while a smaller count of lower- and higher-order relations remains insignificant. The experimental method was selected to ensure that every element was taken into account simultaneously and evaluated for its impact on the response variable. Figure 7 shows the standardized effect of A (temperature), B (modifier), and AB (their interaction), where the distance from the reference line indicates their effect on the response variable. The distance of the modifier content, i.e., B, was greater than the distance of the temperature (A) and their combined effect (AB) from the reference line, which implied that the modifier content (B) was more effective than the temperature (A) and their combined effect (AB). Figure 7 highlights that, practically, the individual effect of the modifier would be greater than the temperature and their combined effect. Figure 8, the main effects plot for MR, focuses on the individual effects of the temperature and modifier of MR. The temperature effect for two levels, high temperature (40 °C) and low temperature (25 °C) plotted against the mean MR values, demonstrated an indirect relationship, as

displayed by the slope of the line (moderate change), i.e., an increase in the temperature from 25 °C to 40 °C resulted in a decline in the MR values, as an increase in the temperature led to an increase in the viscous behavior and a decrease in the stiffness of bitumen; hence, the probability of the permanent deformation was increased. Similarly, the two modifier concentrations, i.e., 0% and 6% (optimum), plotted against the mean MR values gave a direct relationship, as depicted by the slope of the line (abrupt change), i.e., a rise in the modifier content from 0% to 6% improved the compaction and interlocking of aggregates in bitumen due to the filling of pores with the NS particles; this resulted in a rise in the MR value and, ultimately, enhanced performance of the modified specimens. The two-way factorial design involves only two inputs, i.e., upper and lower limits in both modifiers and temperatures, which are connected without any third point (intermediate point) in between, ultimately resulting in a linear relationship. However, it is also pertinent to mention that the temperature effect showing an indirect linear relationship and the modifier illustrating a direct linear relationship demonstrated only a trend line and not a linear relationship. The Pareto chart for MR of 4.5% SBS with varying amounts of the NS-modified HMA are presented in Figure 9. The factors and their interactions have an influence on how the mean response is assessed. The Pareto chart also provides the relative significance of the factor impact, the combined effects of all the variables or their standardized effects, on the mean response at the chosen level of significance (95% confidence interval of 5% t-critical value). The reference line on the chart signified the importance of bars crossing it and the unimportance of bars not doing so. The temperature, modifiers, and their interactions are shown in Figure 9 as having an impact on MR, with bars passing the t-critical line. MR in the Pareto chart was influenced by each of these factors. The Pareto chart also revealed that the effect of the modifier content was greater than that of the temperature and their combined effect. The cube plot for MR of the SBS- and NS-modified HMA is illustrated in Figure 10. The plot shows that at 25 °C with the specimen 4.5% SBS + 6% NS, MR was highest, whereas at 40 °C with the specimen 4.5% SBS + 0% NS, MR was lowest. HMA had a lower MR at 40 °C with the specimen 4.5% SBS + 0% NS due to the material being flexible (limited bonding between aggregates and bitumen) and experiencing larger stresses at high temperatures. The material gave an enhanced MR for low temperatures with the highest modifier content because it stiffened with less strain. Moreover, MR changed considerably with low modifier content and temperature.

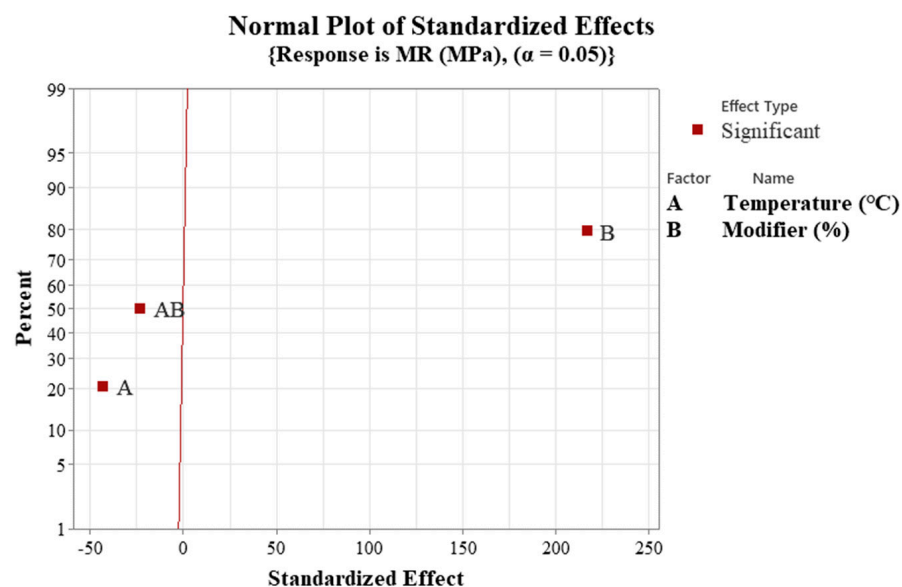


Figure 7. Normal plot for MR of SBS/NS-modified HMA specimens.

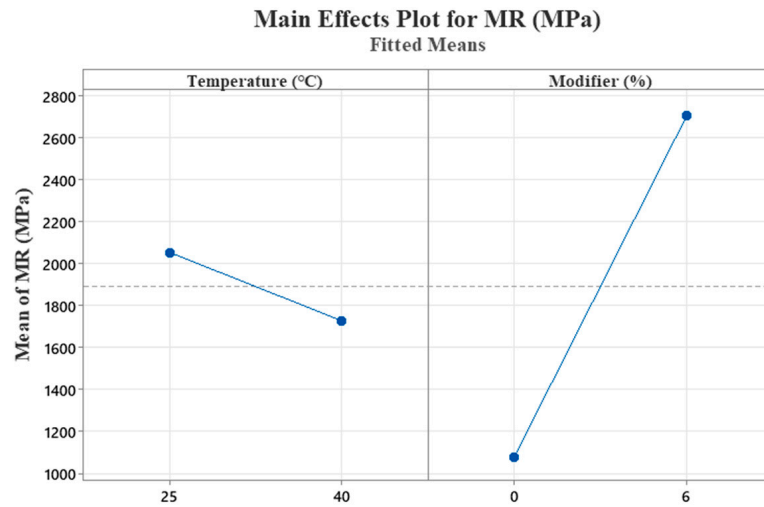


Figure 8. Main effects plot for MR of SBS/NS-modified HMA specimens.

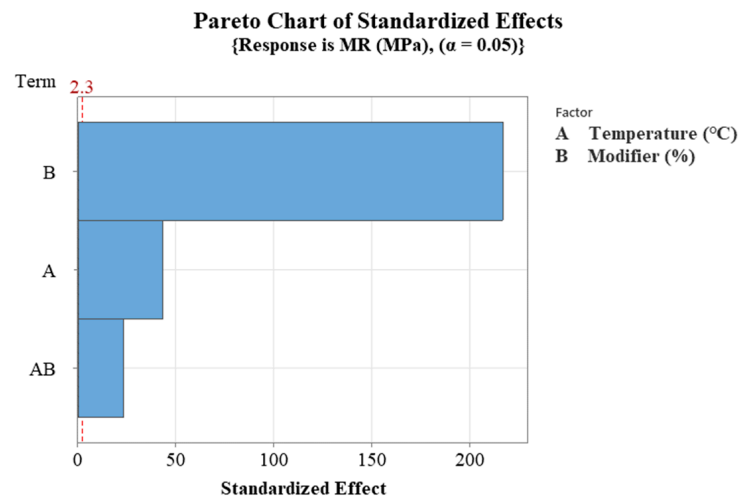


Figure 9. Pareto chart for MR of SBS/NS-modified HMA specimens.

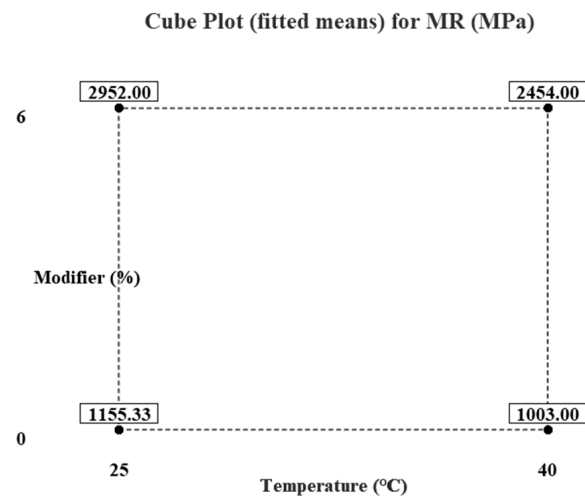


Figure 10. Cube plot for MR of SBS/NS-modified HMA specimens.

As a result, it was demonstrated that MR of the HMA specimens was noticeably affected by the temperature, modification with constant 4.5% SBS, and different percentages of NS-modified HMA. The desirable MR values may be interpolated using the contour plot

depending on a variety of parameters depicted in Figure 11. The MR surface plot of 4.5% SBS with different contents of NS-modified HMA at the lowest and highest temperature levels and modifier are presented in Figure 12. A constant value of 4.5% SBS and different percentages of 2%, 4%, 6%, and 8% NS were used. MR was inversely related to the temperature and directly related to the modifier percentages. These lines, which might be thought of as a topographical map, displayed contours of equal MR in the plot. The curve of the line illustrated the relationship between the temperature and modifier at the lowest and highest levels. Keeping temperature constant, the interpretation of the plot was comparable to 4.5% SBS and 2%, 4%, 6%, and 8% percentages of the NS-modified HMA for the MR values. The MR value may be predicted for each content of the modifier. The easiest method to calculate MR is to draw a line across the contour plot adjacent to the modifier axis. For every point in the temperature axis, a line adjacent to the vertical axis may be drawn from the same modifier percentage to get MR.

Contour Plot of MR (MPa) vs. Modifier (%), Temperature (°C)

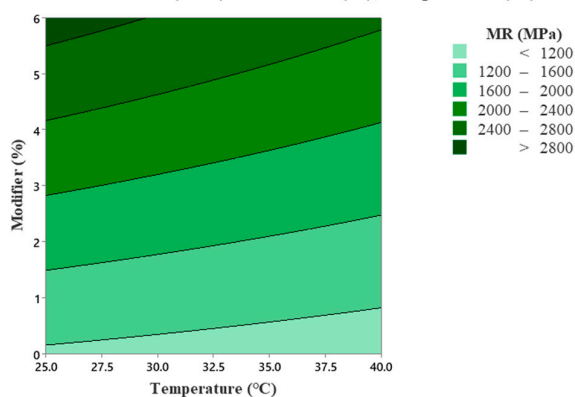


Figure 11. Contour plot for MR of SBS/NS-modified HMA specimens.

Surface Plot of MR (MPa) vs. Modifier (%), Temperature (°C)

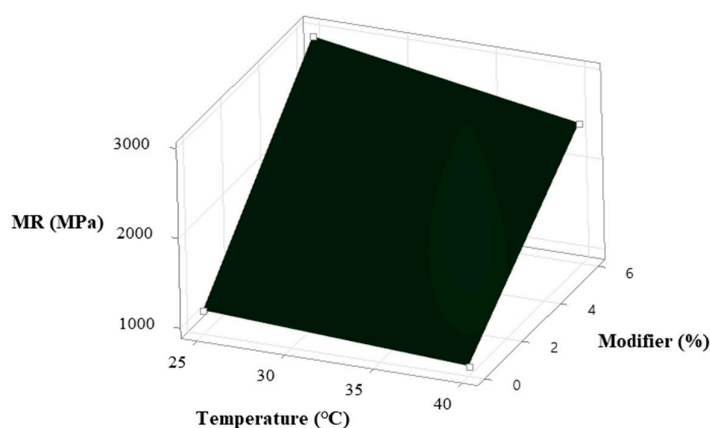


Figure 12. Surface plot for MR of SBS/NS-modified HMA specimens.

Figure 12 provides a 3D depiction of the response variable MR vs. modifier and temperature with 4.5% SBS and 2%, 4%, 6%, and 8% percentages of the NS-modified HMA. MR may be projected by establishing an imaginary line from the required modifier and temperature to get the required MR. Results not calculated in the tests can be seen in Figure 12, which shows that MR was enhanced with a decrease in the temperature and was reduced as the modifier content was decreased.

3.6. MEP

Rutting of SBS/NS-modified HMA specimens was predicted by new predictive equations derived by the MEP strategy [31–35] to address computationally difficult problems. Individual MEPs linearly encode complex computer programs. MEP is used to estimate the rutting potential for various nano-particle (NS) contents, accelerating the utilization of nano-materials and polymers in the civil engineering industry. The capacity of MEP to encode many equations (chromosomes) may be used to combine them into a single program. The final replication of the issue is picked from among the finest of the chosen chromosomes. Unlike other machine learning (ML) methods, MEP does not demand that the final model be known beforehand.

During the MEP evolutionary process, the ultimate expression's mathematical constraints are examined and abolished. The MEP decoding procedure is significantly easier as compared to other ML methods. Additionally, despite the many advantages that MEP has over other evolutionary algorithms, there are still limits to how it may be used in civil engineering. Utilizing MEP is beneficial in cases where the ultimate expression's ambiguity is not immediately apparent, such as in material engineering circumstances where a small modification in a bitumen design property will have a big influence on HMA resilience and rutting. In MEP, a linear chromosome has numerous solutions, which enables the program to predict the result by looking at a larger variety of potential sites. The subpopulation size was set to 100 for both cycles with 4.5% SBS and varying amounts of NS-modified HMA to begin the MEP modeling.

Table 6 presents the chosen hyperparameters for this MEP model. To create a clear and concise final model, the basic mathematical operations of division, subtraction, addition, multiplication, square root, power, absolute, X^2 , and Log10 were considered. How accurate the model is before the process is ended depends on how many generations were utilized to construct it. A program with more generations would result in a better model with fewer errors.

Table 6. MEP parameters for modeling rutting of modified HMA specimens.

MEP Hyperparameter	Modified HMA
Number of subpopulations	10
Subpopulation size	100
Code length	50
Crossover probability	0.9
Mutation probability	0.01
Crossover type	Uniform
Number of generations	1000
Total runs	10

The combination that produced the best outcomes of many combinations was selected. It is important to note that a model's precision is influenced by how long it takes for a new one to be generated. The model develops independently once new variables are included in the setup. On the other hand, this research set 1000 generations as the model's development endpoint, which indicated that fitness function varied with less than 5% uncertainty. Equation (1) is the MEP expression to calculate rutting of 4.5% constant SBS with 2%, 4%, 6%, and 8% NS-modified HMA specimens. R^2 values for the validation data and testing data of the MEP model of the SBS/NS-modified HMA specimens were 95.93% and 94.96%, as demonstrated in Figures 13 and 14, respectively.

$$\text{Rut} = [\log_{10} \{a + (b \times a)\} \times \log_{10} c] - [b \times \{d - (b \times a)\} \times (N \times \log_{10} c)] \quad (1)$$

where

$$a = \frac{N + P}{\sqrt{P}}$$

$$b = \frac{\sqrt{(\sqrt{P})}}{N + P^N}$$

$$c = \sqrt{(\sqrt{P})}$$

$$d = \sqrt{P}$$

$N = NS\%$

$P = \text{cycles}$

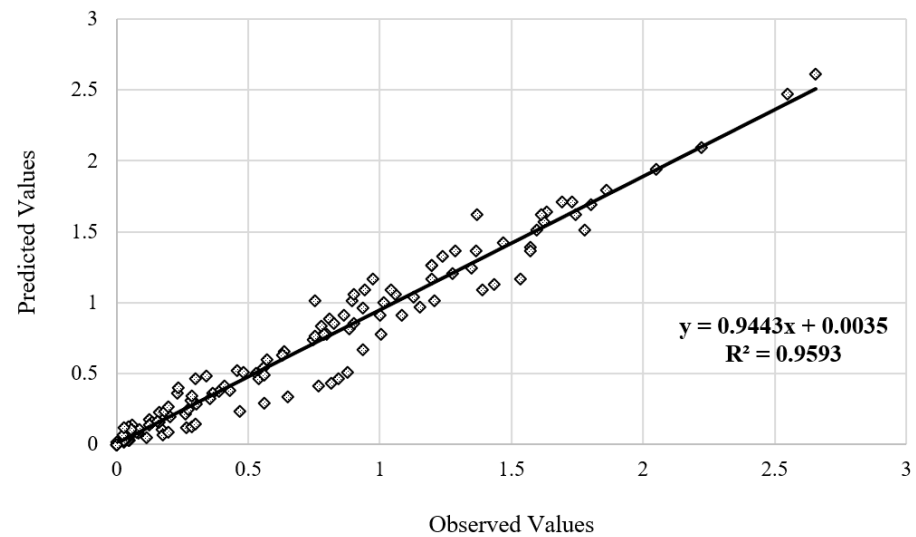


Figure 13. Validation data plot of SBS/NS-modified HMA specimens.

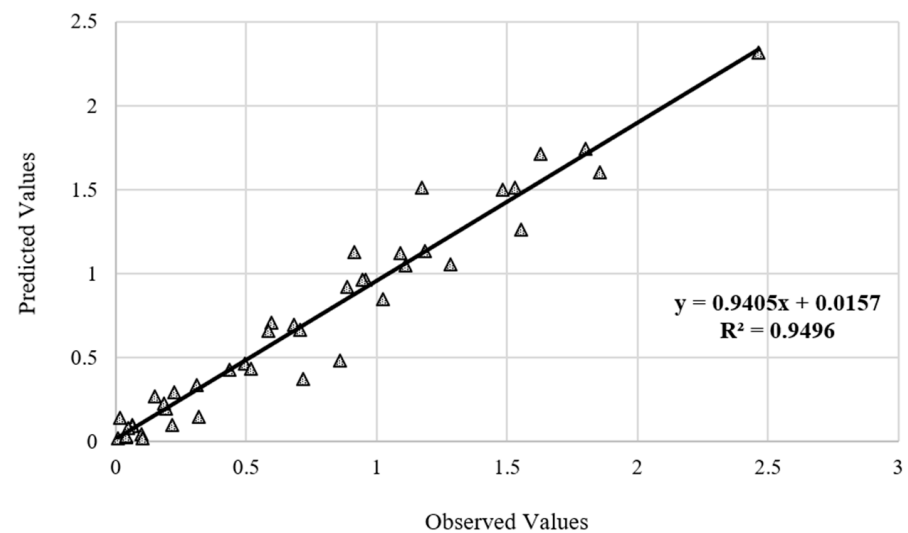


Figure 14. Testing data plot of SBS/NS-modified HMA specimens.

4. Conclusions

The objective of this study was to assess the combine effect of SBS and NS with regard to ITS, stiffness, and rutting using the ITS test, MR test, and WTT. After testing different specimens and comparing their obtained results, the following points are concluded:

- The results showed that the SBS- and NS-modified specimens exhibited enhanced performance against the permanent deformation. The rut resistance was improved by 56% in the modified specimens as compared to the control specimen.
- The SBS- and NS-modified specimens had a higher rate of ITS compared to the control specimen. The results concluded that the use of NS along with SBS had significant effects on the moisture resistance, increasing it by 18%.
- The rise in the percentage of NS against SBS demonstrated a good increase in the stiffness modulus compared to the control specimen. MR had higher values at low temperatures while displaying lower values at higher temperatures. The maximum improvement in the modified HMA specimens was recorded at 1.55 times that of the control specimen.
- The importance of the modifier materials was examined via a two-way factorial design, which verified the experimental outcomes. The results uncovered the significance of the input variables, i.e., modifiers and variables, on the response variable (MR).
- To verify the performance of the MEP model for the rutting potential of the modified specimens, the projected values and experimental values were compared. After the regression analysis, the result revealed a good relation/connection with the experimental results. The optimum combination of SBS and NS was declared at 4.5% and 6%, respectively.
- This study can be applied to real-world road projects to improve the rut resistance of pavements and reduce the maintenance and rehabilitation of asphalt pavements, thus improving the life span of roads. Further improvement in this field can be achieved by carrying out the microstructure analysis of the NS- and SBS-modified asphalt specimens and their performance-based studies, especially at low temperatures. In addition, chemical and rheological testing are also recommended.

Author Contributions: I.K.: Conceptualization; methodology; investigation; validation; writing—original draft. A.W.K.: Conceptualization; methodology; investigation; validation; writing—original draft. A.B.: Conceptualization; methodology; investigation; validation; formal analysis; resources; writing—original draft; writing—review and editing. S.K.: Investigation; validation; writing—original draft. A.E.: Investigation; validation; writing—original draft. All authors have read and agreed to the published version of the manuscript.

Funding: This research received no external funding.

Data Availability Statement: Not applicable.

Conflicts of Interest: The authors declare no conflict of interest.

References

1. Ghanoon, S.A.; Tanzadeh, J.; Mirsepahi, M. Laboratory evaluation of the composition of nano-clay, nano-lime and SBS modifiers on rutting resistance of asphalt binder. *Constr. Build. Mater.* **2020**, *238*, 117592. [[CrossRef](#)]
2. Ahmed, T.A.H. Investigating the Rutting and Moisture Sensitivity of Warm Mix Asphalt with Varying Contents of Recycled Asphalt Pavement. Ph.D. Thesis, The University of Iowa, Iowa City, IA, USA, 2014.
3. Zhu, T.; Ma, T.; Huang, X.; Wang, S. Evaluating the rutting resistance of asphalt mixtures using a simplified triaxial repeated load test. *Constr. Build. Mater.* **2016**, *116*, 72–78. [[CrossRef](#)]
4. Binder, L.; Wax, C.; Oil, C.; Ho, T.; Le, M. Feasibility and sustainable performance of RAP mixtures with low-viscosity binder and castor wax-corn oil rejuvenators. *Buildings* **2023**, *13*, 1578.
5. Cristescu, N.D.; Craciun, E.; Soós, E.; Crc, H. *Mechanics of Elastic Composite*; Chapman & Hall/CRC: Boca Raton, FL, USA, 2003.
6. Yildirim, Y. Polymer modified asphalt binders. *Constr. Build. Mater.* **2007**, *21*, 66–72. [[CrossRef](#)]
7. Shafabakhsh, G.; Rajabi, M. The fatigue behavior of SBS/nanosilica composite modified asphalt binder and mixture. *Constr. Build. Mater.* **2019**, *229*, 116796. [[CrossRef](#)]

8. Izzi, N.; Abozed, A.; Breem, S.; Alattug, H.N.M.; Hamim, A.; Ahmad, J. The effects of moisture susceptibility and ageing conditions on nano-silica/polymer-modified asphalt mixtures. *Constr. Build. Mater.* **2014**, *72*, 139–147. [[CrossRef](#)]
9. Sohel, S.; Singh, S.K.; Ransinchung, G.D.R.N.; Ravindranath, S.S. Effect of property deterioration in SBS modified binders during storage on the performance of asphalt mix. *Constr. Build. Mater.* **2020**, *272*, 121644. [[CrossRef](#)]
10. Bala, N.; Napiah, M.; Kamaruddin, I. Effect of nanosilica particles on polypropylene polymer modified asphalt mixture performance. *Case Stud. Constr. Mater.* **2018**, *8*, 447–454. [[CrossRef](#)]
11. Xia, T.; Chen, X.; Xu, J.; Li, Y.; Zhang, A. Influence of hydrophilic nanosilica premixing method on the property of isocyanate-based polymer modified bitumen. *Constr. Build. Mater.* **2021**, *275*, 122174. [[CrossRef](#)]
12. Ashish, P.K.; Singh, D. Use of nanomaterial for asphalt binder and mixtures: A comprehensive review on development, prospect, and challenges. *Road Mater. Pavement Des.* **2021**, *22*, 492–538. [[CrossRef](#)]
13. Izzi, N.; Ibrahim, D.; Nazrul, A.; Ibrahim, H.; Atmaja, S.; Rosyidi, P.; Abdul, N. Engineering characteristics of nanosilica/polymer-modified bitumen and predicting their rheological properties using multilayer perceptron neural network model. *Constr. Build. Mater.* **2019**, *204*, 781–799. [[CrossRef](#)]
14. Zarei, M.; Salehikalam, A.; Tabasi, E.; Naseri, A.; Worya, M. Pure mode I fracture resistance of hot mix asphalt (HMA) containing nano-SiO₂ under freeze–thaw damage (FTD). *Constr. Build. Mater.* **2022**, *351*, 128757. [[CrossRef](#)]
15. Mashaan, N.; Chegenizadeh, A.; Nikraz, H. Performance of PET and nano-silica modified stone mastic asphalt mixtures. *Case Stud. Constr. Mater.* **2022**, *16*, e01044. [[CrossRef](#)]
16. Enieb, M.; Diab, A. Characteristics of asphalt binder and mixture containing nanosilica. *Int. J. Pavement Res. Technol.* **2017**, *10*, 148–157. [[CrossRef](#)]
17. Miguel, J.; Crucho, L.; Manuel, J.; Dias, S. Mechanical performance of asphalt concrete modified with nanoparticles: Nanosilica, zero-valent iron and nanoclay. *Constr. Build. Mater.* **2018**, *181*, 309–318. [[CrossRef](#)]
18. ASTM D2726/D2726M-17; Standard Test Method for Bulk Specific Gravity and Density of Non-Absorptive Compacted Asphalt Mixtures 1. ASTM International: West Conshohocken, PA, USA, 2021; pp. 7–10.
19. Saltan, M.; Terzi, S.; Karahancer, S. Examination of hot mix asphalt and binder performance modified with nano silica. *Constr. Build. Mater.* **2017**, *156*, 976–984. [[CrossRef](#)]
20. Yang, J.; Tighe, S. A review of advances of nanotechnology in asphalt mixtures. *Procedia-Soc. Behav. Sci.* **2013**, *96*, 1269–1276. [[CrossRef](#)]
21. AS 2891; Methods of Sampling and Testing Asphalt—Methods 13.1: Determination of Resilient Modulus of Asphalt—Indirect Tensile Method. Standards Australia: Sydney, Australia, 1995.
22. D6931; Standard Test Method for Indirect Tensile (IDT) Strength of Asphalt Mixtures. ASTM International: West Conshohocken, PA, USA, 2017.
23. Drews, A. D5-95; Standard Test Method for Penetration of Bituminous Materials. ASTM International: West Conshohocken, PA, USA, 1998; pp. 47–49.
24. D36; Standard Test Method for Softening Point of Bitumen (Ring-and-Ball Apparatus). ASTM International: West Conshohocken, PA, USA, 2009.
25. Taherkhani, H.; Afroozi, S. The properties of nanosilica-modified asphalt cement. *Pet. Sci. Technol.* **2018**, *34*, 1381–1386. [[CrossRef](#)]
26. D6926; Practice for Preparation of Bituminous Specimens Using Marshall Apparatus. ASTM International: West Conshohocken, PA, USA, 2010.
27. Nguyen, H.P.; Cheng, P.; Nguyen, T.T. Properties of stone matrix asphalt modified with polyvinyl chloride and nano silica. *Polymers* **2021**, *13*, 2358. [[CrossRef](#)]
28. Obaid, H.A. Characteristics of warm mixed asphalt modified by waste polymer and nano-silica. *Int. J. Pavement Res. Technol.* **2021**, *14*, 397–401. [[CrossRef](#)]
29. Szydło, A.; Mackiewicz, P. Asphalt mixes deformation sensitivity to change in rheological parameters. *J. Mater. Civ. Eng.* **2005**, *17*, 1–9. [[CrossRef](#)]
30. Szydło, A.; Mackiewicz, P. Verification of bituminous mixtures' rheological parameters through rutting test. *Road Mater. Pavement Des.* **2002**, *4*, 423–438. [[CrossRef](#)]
31. Sun, L.; Xin, X.; Ren, J. Asphalt modification using nano-materials and polymers composite considering high and low temperature performance. *Constr. Build. Mater.* **2017**, *133*, 358–366. [[CrossRef](#)]
32. Montgomery, D.C. Experimental design for product and process design and development. *J. R. Stat. Soc. Ser. D Stat.* **1999**, *48*, 159–177. [[CrossRef](#)]
33. Mee, R. *A Comprehensive Guide to Factorial Two-Level Experimentation*; Springer Science & Business Media: Berlin/Heidelberg, Germany, 2009.
34. Broota, K.D. *Experimental Design in Behavioural Research*; New Age International: Dhaka, Bangladesh, 1989.
35. Zahid, A.; Ahmed, S.; Irfan, M. Experimental investigation of nano materials applicability in Hot Mix Asphalt (HMA). *Constr. Build. Mater.* **2022**, *350*, 128882. [[CrossRef](#)]

Disclaimer/Publisher's Note: The statements, opinions and data contained in all publications are solely those of the individual author(s) and contributor(s) and not of MDPI and/or the editor(s). MDPI and/or the editor(s) disclaim responsibility for any injury to people or property resulting from any ideas, methods, instructions or products referred to in the content.